



HAL
open science

Three Dimensional Trajectory Generation for an Autonomous Plane

Djaber Boukraa, Yasmina Bestaoui, Naoufel Azouz

► **To cite this version:**

Djaber Boukraa, Yasmina Bestaoui, Naoufel Azouz. Three Dimensional Trajectory Generation for an Autonomous Plane. *International Review of Aerospace Engineering*, 2008, 1 (4), pp.355-365. hal-00647285

HAL Id: hal-00647285

<https://hal.science/hal-00647285>

Submitted on 19 Apr 2024

HAL is a multi-disciplinary open access archive for the deposit and dissemination of scientific research documents, whether they are published or not. The documents may come from teaching and research institutions in France or abroad, or from public or private research centers.

L'archive ouverte pluridisciplinaire **HAL**, est destinée au dépôt et à la diffusion de documents scientifiques de niveau recherche, publiés ou non, émanant des établissements d'enseignement et de recherche français ou étrangers, des laboratoires publics ou privés.

Three Dimensional Trajectory Generation for an Autonomous Plane

Djaber Boukraa¹, Yasmina Bestaoui², Naoufel Azouz³

Abstract – A 3D optimal trim trajectories planner algorithm for an autonomous plane is presented in this paper. This planner can generate a sequence of 3D elementary trajectories for a set of predefined waypoints in space. The proposed algorithm uses a sequence of five elementary trim trajectories to generate a three dimensional global trajectory in space. The trim property reduces significantly the complexity of the dynamical model and thus the resolution of the trajectory planning and tracking problems. This approach is based on the Bang-Zero-Bang strategy, taking into account the state and inputs constraints due to the vehicle dynamics, flight envelope and the actuators limitations. In this study, we demonstrate that this strategy satisfies the necessary optimality condition of Pontryaguin.

Keywords: Autonomous plane, Trajectory generation, Trim conditions

I. Introduction

Giving Unmanned Aerial Systems a decisional autonomy requires the development of control and decision methods to execute various operations during a mission, in particular the case with limited communications between the operator and the Unmanned Aerial Vehicle (UAV) or the case of dangerous or dull missions. The aerial vehicle must be able to follow the predefined flight plan, but also to generate a new flight plan in reaction to events occurring during the actual mission which can invalidate the actual flight plan. Trajectory planning is an optimization problem which generates an optimal trajectory between two configurations in the state space, considering a given performance index (time, energy or distance). Its feasibility depends on the choice of the optimization method, the performance index and a number of constraints from various nature, the latter depend essentially on the vehicle itself (architecture, dynamics and actuation modes) and the environment in which the vehicle moves (endurance, airspeed, altitude, landing and takeoff modes ...). Existing approaches in the literature do not deal with the general problem of the trajectory generation, but consider only some aspects e.g. the case of a single aerial vehicle moving in a static environment and without obstacles (free flight) [1]-[2], the cooperation between a vehicle's formation moving in a common space [3]-[4] or the problem of collision and obstacles avoidance [5]-[6].

In general, trajectory planning techniques can be classified in three groups: techniques based on the optimal control theory, on the flatness theory and the probabilistic approaches.

- The optimal trajectory can be found by minimizing a given performance index (execution time, power consumption, distance

covered...) and taking into account some dynamic and kinematic constraints [7]-[8].

- Differential flatness is a structural property of a class of dynamical systems, where all the state and input variables are expressed as functions of a specific variable and its derivatives; this variable being called the flat output. This property can be used to simplify the resolution of a planning problem when an explicit characterization of the trajectories is necessary. There is not a systematic method to find the flat output. However, some references made it possible to establish a specific criterion to determine the flatness of some classes of systems [9]-[11].
- In front of the difficulty to generalize the use of analytical methods, heuristic approaches were developed as the techniques of Road Map and Rapidly Exploring Random Tree [12]-[13]. These techniques use in general a set of primitives used to build the segments of the global way at random. If a segment is feasible (obstacle avoidance) then it is added to the tree of the possible ways. The algorithm continues the tree extension until it reaches the final configuration. The disadvantage of these probabilistic approaches is that the existence of a feasible solution with a probability one is guaranteed only with an unlimited computing time (tends towards the infinite).

Other simpler approaches in the literature use the Dubin's principle [14] considering the shortest way with limited curvature for a vehicle moving in 2D. He showed that between two specified points in a plan the shortest way can be built from a sequence of circular and straight lines, by using a Bang-Zero-Bang strategy. Yang [6] uses this idea to generate feasible trajectories by taking account of the kinematics constraints, where he proposes an algorithm seeking the optimal positions

of circles and line segments. Chandler [15] places the circles in the junctions between the line segments generated by the Voronoï Diagram. Anderson in [16] proposes an algorithm for the optimal trajectory on the horizontal plan, from a set of waypoints with constant altitude, using two types of elementary trajectories: circular and straight lines. His approach can only generate the trajectory in the case of navigation (lateral) mode. In the case of an aerial vehicle these approaches can be applied directly by considering a constant airspeed and altitude and using two elementary trajectories: the horizontal steady wings level and the horizontal turning flight

Our approach is partially inspired from Dubin's work, the idea is to use the straight and circular lines to construct the optimal sequence of trajectories (global optimality), checking the Pontryaguin Maximum Principle (PMP) for elementary trajectories optimality (local optimality) [17]-[19]. It is a generalization of the approach presented in [16]. Our trajectory planner can generate a three dimensional trajectory in space, by adding the climb/descent steady wings level flights and the vertical helices to the initial trim elementary trajectories (horizontal steady wings level and horizontal turning flight). To reduce the complexity of the problem, we will use only the trim trajectories as primitives to generate the global trajectory, the non trim trajectories case will not be treated here. Several scenarios can be considered according to the mission specifications. For example, in the case of Unmanned Aerial Vehicles formation, the trajectory length must be equal to the segment between the waypoints, by opposition to the case of a free flight, where the objective of the passage by a waypoint is to avoid an obstacle or a prohibited area. More details on this point can be found in [16] which deals with three different scenarios of passage by a waypoint.

In this paper, we are interested by the case of minimum time i.e. it is not necessary that the aerial vehicle passes exactly by the waypoint, but has only to reach his neighbourhood.

This paper consists of four sections. Section 2 presents a trajectory planner based on a Bang-Zero-Bang strategy, using a set of trim trajectories as elementary trajectories. Then, we demonstrate that this strategy satisfies the optimality necessary condition of Pontryaguin. In section 3, two examples of scenarios with some comments and remarks are presented. Finally some concluding remarks are given in section 4.

II. Trim Trajectories Planner

As usual in Aeronautics [20], three reference frames are considered in the derivation of the kinematics and dynamics equations of motion. These are the Earth fixed frame R_f , the body fixed frame R_m and the wind frame R_w . The position and orientation of the vehicle should

be described relative to the inertial reference frame while the linear and angular velocities $V = (u \ v \ w)^T$; $\omega = (p \ q \ r)^T$ of the vehicle should be expressed in the body-fixed coordinate system. The origin C of R_m coincides with the center of gravity of the vehicle. Its axes $(X_c \ Y_c \ Z_c)$ are the principal axes of symmetry when available. They must form a right handed orthonormal frame. The position of the vehicle C in R_f can be described by:

$\eta_1 = (x \ y \ z)^T$ while the orientation is given by $\eta_2 = (\phi \ \theta \ \psi)^T$ with ϕ Roll, θ pitch and ψ Yaw angles. The orientation matrix R is given by

$$R = \begin{pmatrix} c\psi c\theta & -s\psi c\theta + c\psi s\theta s\phi & s\psi c\theta + c\psi s\theta c\phi \\ s\psi c\theta & c\psi c\theta + s\psi s\theta s\phi & -c\psi c\theta + s\psi s\theta c\phi \\ -s\theta & c\theta s\phi & c\theta c\phi \end{pmatrix}$$

where $c\theta = \cos(\theta)$ and $s\theta = \sin(\theta)$. This description is valid in the interval $-\frac{\pi}{2} < \theta < \frac{\pi}{2}$. A singularity of this

transformation exists for $\theta = \frac{\pi}{2} \pm k\pi$; $k \in \mathbb{Z}$.

The kinematics of the UAV can be expressed in the following way:

$$\begin{pmatrix} \dot{\eta}_1 \\ \dot{\eta}_2 \end{pmatrix} = \begin{pmatrix} R & 0_{3 \times 3} \\ 0_{3 \times 3} & J(\eta_2) \end{pmatrix} \begin{pmatrix} V \\ \Omega \end{pmatrix}$$

$$\text{where } J(\eta_2) = \begin{pmatrix} 1 & s\phi \cdot \tan \theta & c\phi \cdot \tan \theta \\ 0 & c\phi & -s\phi \\ 0 & s\phi / c\theta & c\phi / c\theta \end{pmatrix}$$

In Aeronautics, trim trajectories have a significant place. Under the trim condition the vehicle motion is uniform in the body fixed frame. The trim trajectories have the advantage of facilitating the planning and control problems. A linear control technique could be sufficient to stabilize the vehicle in the neighbourhood of trim conditions. Another advantage is that the aerodynamic coefficients which are variable in time and space become stationary under this condition and their identification becomes easier.

II.1. Trim Conditions Determination Algorithm

The vehicle configuration in space is defined by its linear and angular velocities and the pitch and roll angles. If we refer to some simplifying assumptions, neglecting the ground curvature and the air density variation with altitude, a vector of eight state variables $(V, \alpha, \beta, p, q, r, \theta, \phi)^T$ would be enough to parameterize any trim trajectory in space.

II.2. Trajectory Planner

B. Performance index

In the case of a trim trajectory, the external forces and moments are constant or equal to zero. The aim is to determine the trim conditions i.e. all accelerations vanish ($\dot{V}, \dot{\alpha}, \dot{\beta}, \dot{p}, \dot{q}, \dot{r} = 0$). The state and control vectors are determined by the resolution of a nonlinear equations system. Thus, we can formulate a numerical optimization problem seeking to minimize all accelerations. The performance index chosen in the algorithm is the sum of the squares of accelerations:

$$J = (\dot{V}^2 + \dot{\alpha}^2 + \dot{\beta}^2 + \dot{p}^2 + \dot{q}^2 + \dot{r}^2) \quad (1)$$

B. Constraints

The algorithm must take account of some constraints: under-actuation, flight envelope, trajectory geometry, actuators limitations and environment [17]-[20].

Under-actuation constraints

The autonomous plane has four control inputs: throttle, elevator, aileron and rudder, the number of degrees of freedom being six. Thus we can formulate two equality dynamical differential equations as constraints due to the underactuation.

Flight envelope constraints

In order to guarantee some flight performances and for safety reasons we define a flight envelope. To avoid stalling phenomena, the vehicle airspeed should not be below a value called stalling speed. The maximum available power provided by the engines imposes a maximum limit speed. Limitations on the load factor are imposed to limiting the effort exerted on the structure during the turn and pull up.

Trajectory geometry

The choice of the trajectory geometry (line, circle etc.) imposes kinematics constraints. In [17], we can find two examples of these constraints. The first one is an algebraic relation expressing the pitch angle as function of desired rate of climb (rate of climb constraint). The second example is an algebraic constraint allowing a coordinated turn by expressing the roll angle as function of desired heading rate. This ensures that the vehicle turning without skidding (coordinated turn constraint). These two constraints can be used in any optimization algorithm.

Constraints dues to the actuators limitations

Throttle position is included between zero and maximum power available. The deflection angles of the control surfaces vary between two limits. These limitations can be introduced into any algorithm in form of algebraic inequalities as follows:

$$\begin{aligned} 0 \leq \Pi \leq \Pi_{\max}, \delta_{e\min} \leq \delta_e \leq \delta_{e\max} \\ \delta_{a\min} \leq \delta_a \leq \delta_{a\max}, \delta_{r\min} \leq \delta_r \leq \delta_{r\max} \end{aligned} \quad (2)$$

A. Problem formulation

We consider the vehicle in a trim flight with constant airspeed. The more general trim trajectory is a vertical helices with constants curvature and rate of climb. This trajectory can be described by the following equations:

$$\begin{cases} \dot{x} = A \cos(\psi.t) + B \sin(\psi.t) \\ \dot{y} = -B \cos(\psi.t) + A \sin(\psi.t) \\ \dot{z} = C \end{cases} \quad (3)$$

$$A = V \cos \alpha \cos \beta \cos \theta + V \sin \beta \sin \theta \sin \phi \\ + V \sin \alpha \cos \beta \sin \theta \cos \phi$$

with

$$B = -V \sin \beta \cos \phi + V \sin \alpha \cos \beta \sin \phi$$

$$C = -V \cos \alpha \cos \beta \sin \theta + V \sin \beta \cos \theta \sin \phi \\ + V \sin \alpha \cos \beta \cos \theta \cos \phi$$

We assume that the vehicle is equipped with a control system ensuring the reference trajectory tracking. The role of this system is to maintain the vehicle airspeed V attitude (Euler angles) and aerodynamic angles within their respective desired values:

$$\text{- Airspeed: } \dot{V} = f_V(V_c - V)$$

$$\text{- Attitude: } \dot{\phi} = f_\phi(\phi_c - \phi), \dot{\theta} = f_\theta(\theta_c - \theta), \dot{\psi} = f_\psi(\psi_c - \psi)$$

$$\text{- Aerodynamic angles: } \dot{\alpha} = f_\alpha(\alpha_c - \alpha), \dot{\beta} = f_\beta(\beta_c - \beta)$$

with $f_\psi, f_V, f_\phi, f_\theta, f_\alpha$ et f_β control laws (function of difference between reference $(V_c, \phi_c, \theta_c, \psi_c, \alpha_c, \beta_c)$

and measured values $(V, \phi, \theta, \psi, \alpha, \beta)$) computed by the control system. The state constraints defining the flight envelope are:

$$-\dot{\psi}_{\max} \leq \dot{\psi} \leq \dot{\psi}_{\max}, 0 < V_{\min} \leq V \leq V_{\max}$$

$$\alpha_{\min} \leq \alpha \leq \alpha_{\max}, |\beta| \leq \beta_{\max}, |\phi| \leq \phi_{\max} \quad (4)$$

The constant $\dot{\psi}_{\max}$ is determined by the maximal value of the load factor. Stalling phenomena imposes minimal vehicle airspeed V_{\min} and the maximal value of angle of attack α_{\max} . The available engines power allows determining maximal vehicle airspeed V_{\max} . A last constraint on the state allows maintaining the sideslip angle β in the neighbourhood of zero. To ensure the regularity of the coordinate transformation matrix, we suppose: $\theta \neq \pm \frac{\pi}{2}$.

A trajectory $t\hat{r}(t) = (\hat{x}(t), \hat{y}(t), \hat{z}(t))^T$ is known as dynamically feasible if there exist inputs $\psi_c, \phi_c, \theta_c, V_c, \alpha_c, \beta_c$ such as $tr(t) = t\hat{r}(t)$ for all $t \geq 0$, the dynamics and the constraints (4) being satisfied. The input of the trajectory planner algorithm are the desired airspeed \hat{V} and the waypoints coordinates

$(x, y, z)_i \in R^3$ expressed in the Earth fixed frame:

$$\{\hat{V}, (x, y, z)_1, (x, y, z)_2, \dots, (x, y, z)_n\}.$$

Thus, the trajectory planner equations are given by:

$$\begin{cases} \dot{\hat{x}} = \hat{A} \cos(\hat{\psi}t) + \hat{B} \sin(\hat{\psi}t) \\ \dot{\hat{y}} = -\hat{B} \cos(\hat{\psi}t) + \hat{A} \sin(\hat{\psi}t) \\ \dot{\hat{z}} = \hat{C} \sin u_2 \\ u_1 = \hat{\psi} & |u_1| \leq \dot{\psi}_{\max} \\ u_2 = \hat{\gamma} & |u_2| \leq \gamma_{\max} \end{cases} \quad (5)$$

With

$$\begin{aligned} \hat{A} &= \hat{V} \cos \alpha \cos \beta \cos \theta + \hat{V} \sin \beta \sin \theta \sin \phi \\ &\quad + \hat{V} \sin \alpha \cos \beta \sin \theta \cos \phi \\ \hat{B} &= -\hat{V} \sin \beta \cos \phi + \hat{V} \sin \alpha \cos \beta \sin \phi \\ \hat{C} &= -\hat{V} \cos \alpha \cos \beta \sin \theta + \hat{V} \sin \beta \cos \theta \sin \phi \\ &\quad + \hat{V} \sin \alpha \cos \beta \cos \theta \cos \phi \end{aligned}$$

If we suppose that the trajectories are traversed with a constant airspeed \hat{V} included between V_{\min} and V_{\max} , the initial condition $\hat{r}(0) = r(0)$ and equations (5) guarantee a priori the dynamical feasibility of the trajectory. This trajectory will be generated by resolution of system (5), by the ODE45 MATLAB[®] function (fourth order Runge Kutta method).

We note that if $u_1 = \dot{\psi}_{\max}$, the trajectory generated by (5) is a circle on the right side of the plane where the centre is given by :

$$(x, y, z)_{cent}^T = (\hat{x}, \hat{y}, \hat{z})^T + R_{\min} \cdot (-\sin(\hat{\psi}t), \cos(\hat{\psi}t), 1)^T$$

If $u_1 = -\dot{\psi}_{\max}$, the trajectory generated by (5) is a circle on the left side of the plane where the centre is given by :

$$(x, y, z)_{cent}^T = (\hat{x}, \hat{y}, \hat{z})^T + R_{\min} \cdot (\sin(\hat{\psi}t), -\cos(\hat{\psi}t), 1)^T$$

If $u_2 = +\gamma_{\max}$, the flight path angle is positive (up) and given by : $\dot{H} = V \cdot \sin \gamma_{\max}$

If $u_2 = -\gamma_{\max}$ the flight path angle is negative (down) and given by: $\dot{H} = -V \cdot \sin \gamma_{\max}$.

In this paper, we suppose that there is already an algorithm defining waypoints set and optimizing the segments sequence between the start and target points. This waypoints sequence depends mainly on the nature of mission and the environment in which the aerial vehicle is moving.

B. Dubins curves

In this section we present briefly the Dubins principle [14] in the optimal trajectory generation with a limited curvature for a vehicle moving in a plan [6], [8], [16]. A direct application of this principle is possible in the case a flight at constant altitude with a constant airspeed. If we suppose that the yaw angle is controlled by a

stability augmentation system. Thus, the kinematics equations can be reduced as :

$$\begin{cases} \dot{x} = V \cdot \cos \psi \\ \dot{y} = V \cdot \sin \psi \\ \dot{\psi} = u = K_{\psi} \cdot (\psi_c - \psi) \end{cases} \quad (6)$$

With V the airspeed, ψ the yaw angle, x and y are respectively the north and east UAV positions. These parameters are represented in Fig. 5.

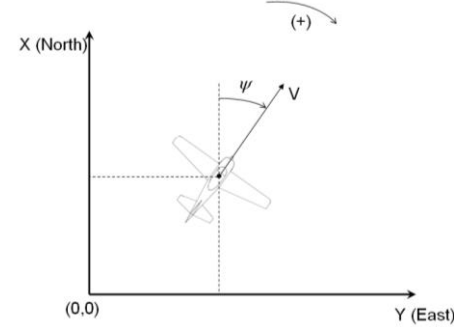


Fig. 1 The directions and orientation used in the case of flight in the horizontal plan.

We assume also a trajectory curvature constraint corresponding to a turn minimal radius R_{\min} . The approach minimizes the trajectory length to go from an initial point p_i to a final point p_f :

$$J(p_i, p_f, u) = \int_0^{t_f} \sqrt{\dot{x}^2(t) + \dot{y}^2(t)} dt \quad (7)$$

Dubins[14] shows that between any two configurations, it is possible to construct the shortest path with a combination of a maximum of three primitives. In each primitive we apply a constant action during a time interval. The primitives and their symbols are represented in Table 2. S indicates a straight line, R and L indicate respectively, the right and left level (sharpest) turn.

Table 1 Dubins primitives and their symbols.

Primitive type	Symbol	Yaw rate $\dot{\psi}$
Straight line	S	0
Right level turn	R	$+\dot{\psi}_{\max}$
Left level turn	L	$-\dot{\psi}_{\max}$

Any extremal trajectory can be indicated by a sequence of three symbols. This sequence corresponds to the order of which the primitives are applied. It is not necessary to have two symbols of a same type consecutively, because they can be reduced to one symbol. Dubins proved that among all the possible sequences only six can be optimal:

$$\{RLR ; LRL ; RSR ; RSL ; LSL ; LSR\} \quad (8)$$

The shortest path between two any configurations can be characterized by one of these sequences. They are called

the Dubins curves. We can allot to each primitive an index which indicates the execution time. In the case of a level turn the index $(\mu, \nu$ or O) indicates the rotation carried out during the application of the primitive. In the case of a straight line the index d indicates the total covered distance during the application of the primitive. With these indexes the sequences will be presented as follows:

$$\left\{ \begin{array}{l} R_\mu L_\nu R_o ; L_\mu R_\nu L_o ; R_\mu S_d R_o ; \\ R_\mu S_d L_o ; L_\mu S_d L_o ; L_\mu S_d R_o \end{array} \right\}$$

Fig. 2 shows these six curves. We note that the index ν must be greater than π .

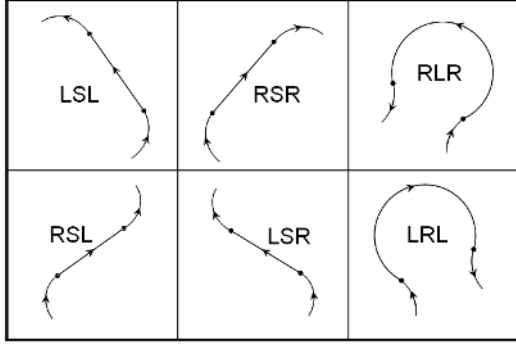


Fig. 2 The six sequences of Dubins.

With these definitions the problem is formulated as follows: being given the points p_i and p_f , which among the sequences in eq. (8) is the shortest? And which are the values of indices of this sequence?

A simple algorithm can answer these two questions, by evaluating for the six sequences, than by choosing the shortest among them, for each segment between two waypoints.

C. Pontryaguin Minimum Principle

We consider the dynamical system state equation

$$\dot{X} = f(X(t), u(t)) \quad (9)$$

with the initial condition $X(0) = X_0$

$f : R^n \times R^m \rightarrow R^n$ being of the class C^1 . Let be

P_0 and P_f two subsets of R^n , and U the limited

controls set $U = \{u \in R^m : |u| \leq u_{\max}\}$ of which the

associated trajectories joining an initial point p_0 of P_0 to

a final point p_f of P_f in finite time $t(u)$. In addition we

define the cost function in the interval $[0, T]$ as:

$$J(t, u) = g(X(T)) + \int_0^T L(X(\tau), u(\tau), \tau) d\tau$$

$g(X(T))$ is the terminal cost:

$$g(X(T)) = \frac{1}{2} \cdot [X(T) - X_T]^T \cdot [X(T) - X_T].$$

The Hamiltonian H is defined by:

$$H(X, u, \lambda, \rho, t) = L(X, u, t) + \lambda^T \cdot f(X, u, t)$$

with $\lambda(\cdot) : [0, T] \rightarrow R^n$ Lagrange multipliers.

Necessary optimality conditions are:

$$H(X^*, u^*, \lambda^*, \rho^*, t) \leq H(X^*, u, \lambda^*, \rho^*, t) \quad \forall t, \forall u \in U \quad (10)$$

$$\dot{X}(t) = \frac{\partial H}{\partial \lambda} \quad (11)$$

$$\dot{\lambda}(t) = - \frac{\partial H}{\partial X} \quad (12)$$

Transversality conditions:

If the final point is not fixed, we have the following transversality condition:

$$\lambda(T) = \frac{\partial g}{\partial X}(T) \cdot \rho \quad (13)$$

With ρ real. Moreover, if the final instant is free, Then

$$H(X^*, u^*, \lambda^*, \rho^*, t) = 0 \quad (14)$$

Extremal Trajectories

Let's define the way path by three points p_{i-1} , p_i and p_{i+1} , see Fig. 3. The projection of segments

$[p_{i-1}p_i]$ and $[p_i p_{i+1}]$ in the horizontal plan gives respectively the segments $[\bar{p}_{i-1}\bar{p}_i]$ and $[\bar{p}_i\bar{p}_{i+1}]$. Let's

define \bar{C} the circle tangent with the two segments $[\bar{p}_{i-1}\bar{p}_i]$ and $[\bar{p}_i\bar{p}_{i+1}]$ of radius

$R_{\min} = V / \dot{\psi}_{\max}$ of which the centre belongs to the bisector of the angle formed by the three waypoints.

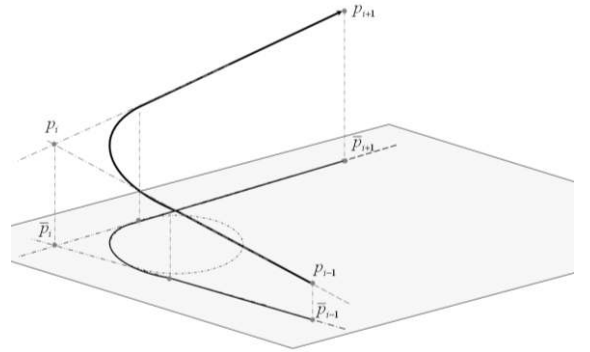


Fig. 3 Trajectory projection in the horizontal plan (x,y).

The trajectory between the points \bar{p}_{i-1} and \bar{p}_{i+1} is constructed as follows:

1- The segment $[\bar{p}_{i-1}\bar{p}_i]$ is followed until \bar{p}_{i1} the intersection point with the circle \bar{C} .

2- Then the arc of circle \bar{C} from \bar{p}_{i1} to \bar{p}_{i2} the

intersection point with the segment $[\bar{p}_i \bar{p}_{i+1}]$.

3- Finally, the segment $[\bar{p}_{i2} \bar{p}_{i+1}]$ is followed until the point p_{i+1} .

The circle \bar{C} is in fact the projection of the vertical helix with constant rate of climb \dot{z} .

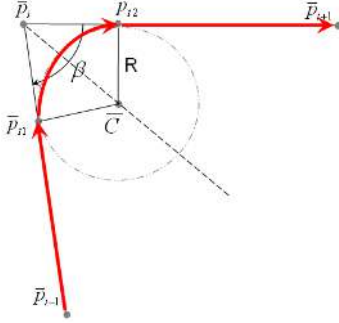


Fig. 4 Time optimal control problem in the new coordinates.

Proposition: The helicoidally trajectory defined previously in fig. 4 is time optimal and allows the transition between the segments $[p_{i-1} p_i]$ and $[p_i p_{i+1}]$.

Proof: Without loss of generality, we can realise coordinate transformation such as the segment $[p_i p_{i+1}]$ is aligned with the axis OY as shown in fig. 4. Let's consider the system:

$$\begin{cases} \dot{x} = A \cos \psi + B \sin \psi \\ \dot{y} = -B \cos \psi + A \sin \psi \\ \dot{z} = V \sin u_1 \\ \dot{\psi} = u_2 \end{cases} \quad (15)$$

With the initial conditions $(x(0), y(0), z(0), \psi(0))^T = (x_0, y_0, z_0, \psi_0)^T$ and the terminal constraint:

$$g(x, y, z, \psi) = \frac{1}{2} (x(T)^2 + (z(T) - z_T)^2 + \psi(T)^2) = 0 \quad (16)$$

This constraint ensures that at the final time T , the projected point in the horizontal point is aligned with the straight line $(\bar{p}_i \bar{p}_{i+1})$ and the final altitude $z(T)$ is equal to z_T . The Hamiltonian of system is given by:

$$H = 1 + \lambda_x (A \cos(\psi) + B \sin(\psi)) + \lambda_y (-B \cos(\psi) + A \sin(\psi)) + \lambda_z V \sin u_1 + \lambda_\psi u_2 \quad (17)$$

According to the condition (10) the partial derivatives of H in the two controls should be equal to zero. The Hamiltonian has a linear form thus the minimization is ensured by the controls saturation taking account of the signs of the Lagrange multipliers λ_z and λ_ψ . The condition (11) is easily verified. The condition (12) results in the following relations:

$$\dot{\lambda}_x = -\frac{\partial H}{\partial x} = 0 \Rightarrow \lambda_x = \text{constant}$$

$$\dot{\lambda}_y = -\frac{\partial H}{\partial y} = 0 \Rightarrow \lambda_y = \text{constant}$$

$$\dot{\lambda}_z = -\frac{\partial H}{\partial z} = 0 \Rightarrow \lambda_z = \text{constant}$$

$$\dot{\lambda}_\psi = -\frac{\partial H}{\partial \psi} = -\lambda_x (-A \sin \psi + B \cos \psi) - \lambda_y (B \sin \psi + A \cos \psi)$$

$$\Rightarrow \dot{\lambda}_\psi = -\frac{\lambda_x}{u_2} (A \cos \psi + B \sin \psi) - \frac{\lambda_y}{u_2} (-B \cos \psi + A \sin \psi) + k$$

The values of constants $\lambda_x, \lambda_y, \lambda_z$ and k are determined by the transversality conditions (the final point is not fixed but it belongs to a subset of \mathcal{R}^n):

$$\Rightarrow \lambda^*(T) = \frac{\partial g}{\partial x} \Big|_T \cdot \rho$$

$$\lambda_x(T) = \frac{\partial g}{\partial x} \Big|_T \cdot \rho_x = \rho_x \Rightarrow \lambda_x = \rho_x$$

$$\lambda_y(T) = \frac{\partial g}{\partial y} \Big|_T \cdot \rho_y = 0 \Rightarrow \lambda_y = 0$$

$$\lambda_\psi(T) = \frac{\partial g}{\partial z} \Big|_T \cdot \rho_\psi = \rho_\psi$$

$$\Rightarrow k = \rho_\psi + \frac{\lambda_x}{u_2} (A \cos \psi(T) + B \sin \psi(T)) +$$

$$\frac{\lambda_y}{u_2} (-B \cos \psi(T) + A \sin \psi(T))$$

$$\lambda_z(T) = \frac{\partial g}{\partial z} \Big|_T \cdot \rho_z = \rho_z \Rightarrow \lambda_z = \rho_z$$

We evaluate the Hamiltonian of the system:

$$H = 1 + \rho_z u_1 + \rho_\psi u_2 + \rho_x (A \cos \psi(T) + B \sin \psi(T))$$

Now, we discuss the dependency of the Hamiltonian of the controls (u_1 and u_2):

If $(\rho_z, \rho_\psi) > (0, 0)$ thus H is minimal for $(u_1, u_2) = (-u_{1\max}, -u_{2\max})$

If $(\rho_z, \rho_\psi) < (0, 0)$ thus H is minimal for $(u_1, u_2) = (u_{1\max}, u_{2\max})$

If $\rho_z > 0$ et $\rho_\psi < 0$ thus H is minimal for $u_1 = -u_{1\max}$ et $u_2 = u_{2\max}$

If $\rho_z < 0$ et $\rho_\psi > 0$ thus H is minimal for $u_1 = u_{1\max}$ et $u_2 = -u_{2\max}$

It thus consists of Bang-Off-Bang control strategy:

$$\begin{cases} u_1 = -\gamma_{\max} & \text{for a descent} \\ u_1 = +\gamma_{\max} & \text{for a climb} \\ u_2 = \dot{\psi}_{\max} & \text{for a right level turn} \\ u_2 = -\dot{\psi}_{\max} & \text{for a left level turn} \end{cases}$$

Now, we suppose that this control strategy is optimal and we find the existence of the Lagrange multipliers

and the real numbers ρ such as the resultant system satisfies the conditions (10)-(14). Integrating eq. (15) we obtain:

$$z = (V \cdot \sin \gamma_{\max}) \cdot t + z_0 \quad (19)$$

$$\psi = \dot{\psi}_{\max} \cdot t + \psi_0 \quad (20)$$

In the same way for $\dot{\lambda}_{\psi}$:

$$\dot{\lambda}_{\psi} = -\frac{\partial H}{\partial \psi} = -\rho_x \cdot (-A \cdot \sin(\dot{\psi}_{\max} \cdot t + \psi_0) + B \cdot \cos(\dot{\psi}_{\max} \cdot t + \psi_0))$$

$$\lambda_{\psi} = -\frac{\rho_x}{\dot{\psi}_{\max}} \cdot (A \cdot \cos(\dot{\psi}_{\max} \cdot t + \psi_0) + B \cdot \sin(\dot{\psi}_{\max} \cdot t + \psi_0)) + k$$

$$\lambda_{\psi}(T) = \rho_{\psi} \Rightarrow$$

$$k = \rho_{\psi} + \frac{\rho_x}{\dot{\psi}_{\max}} \cdot (A \cdot \cos(\dot{\psi}_{\max} \cdot T + \psi_0) + B \cdot \sin(\dot{\psi}_{\max} \cdot T + \psi_0))$$

To satisfy the condition (14):

$$H = 1 + \rho_x \cdot (A \cdot \cos(\dot{\psi}_{\max} \cdot T + \psi_0) + B \cdot \sin(\dot{\psi}_{\max} \cdot T + \psi_0)) + \rho_{\psi} \cdot \dot{\psi}_{\max} - \rho_z \cdot \gamma_{\max} = 0$$

It is thus enough to choose:

$$\rho_x = 1 / (A \cdot \cos(\dot{\psi}_{\max} \cdot T + \psi_0) + B \cdot \sin(\dot{\psi}_{\max} \cdot T + \psi_0))$$

$$\rho_z = 1 / \gamma_{\max} \quad \rho_{\psi} = -1 / \dot{\psi}_{\max} \cdot$$

The existence of the Lagrange multipliers λ_i and the reels ρ_i proves that the Bang-Off-Bang strategy satisfies the optimality conditions of Pontryaguin and consequently the generated trajectory is optimal. **(end of proof)**

Algorithm description

The proposed algorithm allows computing the time parameterized optimal trajectory between two arbitrary points at the same altitude. The algorithm presented here is intended to generate a trajectory for a specified type of missions: monitoring or surveillance mission of geographic area, the area being represented by a point coordinates. We will not consider the constraints due to the traffic. The presence of possible obstacles prohibited areas between the start point (the runway) the target point (monitoring area), requires that the UAV passes by a number of waypoints before reaching the target. The diagram of the algorithm is presented in Fig. 5. It comprises five steps:

1. Initialisation: We introduce the UAV cruise speed and altitude (constants), the runway data (coordinates, direction and altitude), the target and possible waypoints coordinates. We define also the maximal trajectory curvature and rate of climb (descent).

2. Initial climb: One compute the horizontal distance which the UAV must traverse before starting the manoeuvres, than one generates the initial climb trajectory.

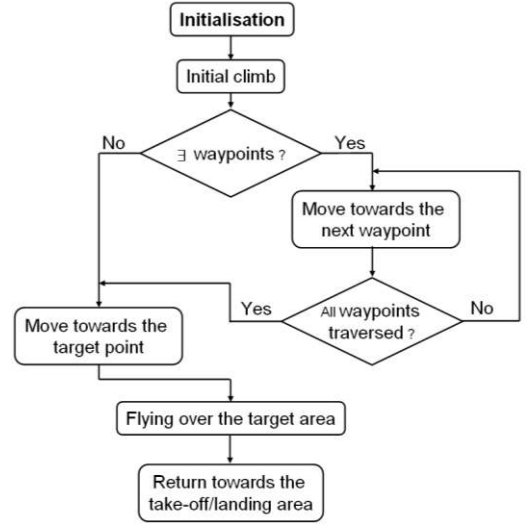


Fig. 5 Diagram of the trajectory planner.

3.a. To move towards the next waypoint: For each waypoint, one determines the direction of turn and the transition times straight/circle/straight, one repeats this operation as many times as the number of waypoints.

3.b. To move towards the target point: in the case when there is no waypoint, one makes one turn to direct towards the target point.

4. Flying over the target area: from the target point coordinates one determines the transition times: straight line/right turn/left turn/right turn. The circle of which belongs the left turn will be traversed several times to allow the sensors in board to carry out the necessary measurements.

5. Return to the landing/take-off area: while leaving the target area, the UAV traverse the same generated trajectory in the opposite direction.

During step 3 the algorithm determines the turn centre position and direction (left or right) from the position of the waypoint. In Fig. 6, the coordinate space is decomposed into four subspaces separated by the direction line of actual waypoint and the perpendicular line to this direction in the horizontal plan. Thus, we distinguish four possible cases. Here, we only present the two cases of a right level turn, the two left turn being symmetric with those.

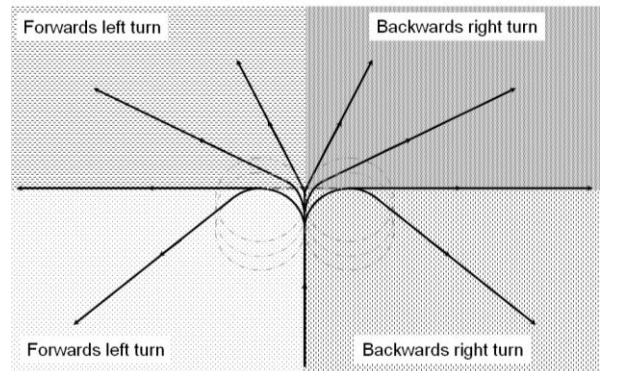


Fig. 6 The four (subspaces) types of turn.

Case of backward right turn

In the case when the next waypoint is rather behind the actual waypoint, the turn (circle) centre and the start point are determined by the actual waypoint coordinates, only the end point depends from the next waypoint coordinates. In fact, it consists to a constraint due to the actual point position. The UAV must approach enough the actual waypoint before starting a new turn. Indeed, the role of a waypoint is to allow the UAV to avoid an obstacle or a prohibited area. Without this constraint the UAV is likely to start a turn towards the next waypoint before reaching the neighbourhood of actual waypoint as we can see in Fig. 7.

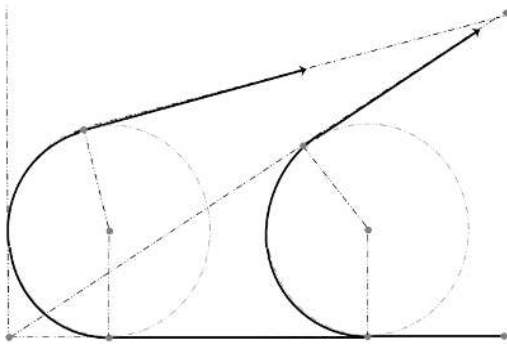


Fig. 7 The two possible cases of turn construction of which the next waypoint is behind the actual one.

Case of a forward right turn

If the next waypoint is rather ahead the actual point, the algorithm computes the turn (circle) centre from the next waypoint coordinates, than it determines the start and end points of the arc of circle.

III. Examples of Mission Profile

IV.1 Simple Profile (no waypoint)

In this section we present two examples of mission, the first one represents a simple mission without any waypoint. The UAV must reach the target area and fly over it. In this case one has only one constraint due to the necessary minimal horizontal distance to be traversed before starting the navigation. The runway coordinates are specified at 0 meters North and 0 meters East with heading angle zero. The target point is chosen at 15 km North and 25 km East. In Fig. 8; the blue curve represents the UAV flight path. Table 3 recapitulates the different phases of the mission with the transitions times between the elementary trajectories.

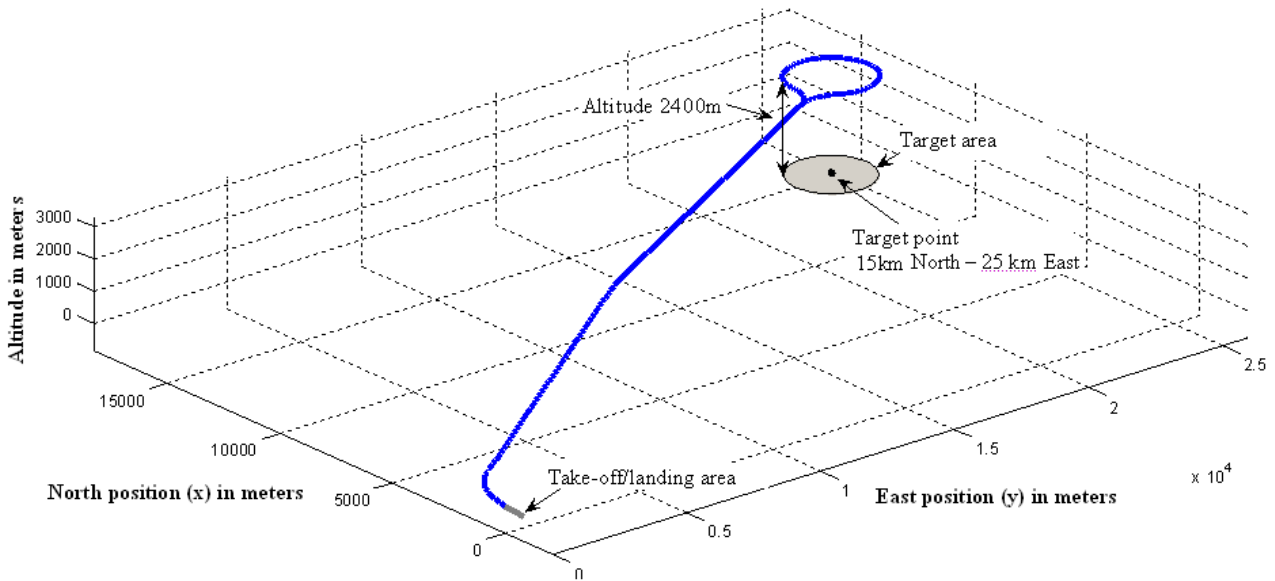


Fig. 8 Example of a simple mission profile (without any obstacle or prohibited area).

Table 3 Different phases of the mission: a simple profile without any waypoint.

Time interval	Tracked trajectory
$t_0 = 0\text{ s}$; $t_1 = 8\text{ s}$	Initial climb with rate 10m/s and initial heading 0 (initial).
$t_1 = 8\text{ s}$; $t_2 = 38\text{ s}$	Right helix towards the target point. Rotation of 60° with rate of yaw of $2^\circ/\text{s}$ and a rate of climb of 10m/s. turn radius of 1432 m.

$t_2 = 38\text{ s}$; $t_3 = 543\text{ s}$	Climb with rate of 10m/s until a time $t_h = 240\text{ s}$ (corresponds to $H=2400\text{ m}$) then a horizontal wings level flight.
$t_3 = 543\text{ s}$; $t_4 = 573\text{ s}$	Horizontal right level turn. Rotation of 60° with yaw rate of $2^\circ/\text{s}$ for surrounding the target point.
$t_4 = 573\text{ s}$; $t_5 = 723\text{ s}$	A horizontal left level turn flight with at least 300° around the target (possibility to carry out several rotations).
$t_5 = 723\text{ s}$; $t_6 = 753\text{ s}$	Right wings level turn. Rotation of 60° to align on the trajectory which carries out towards the take-off/landing area.

IV. 2 Mission with two waypoints

The second example is like the first one except that the UAV must pass by two waypoints before reaching the target area. The two waypoints are respectively 15 km North and 5 km west (-5 km East) for the first and 5 km North and 10 km East for the second.

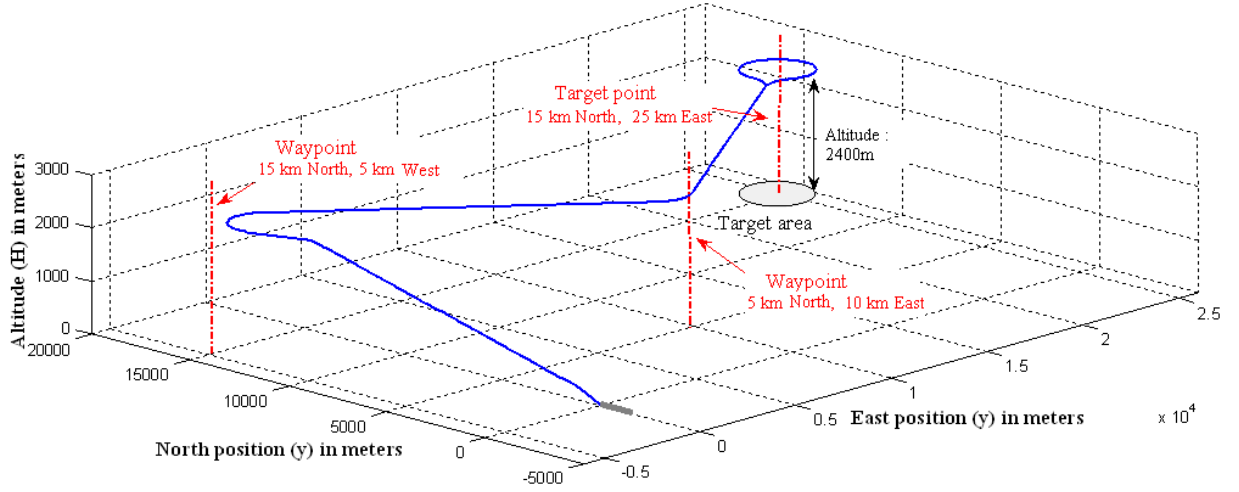


Fig. 9 Example of profile with two waypoints.

Table 4 Different phases of the mission: with two waypoints.

Time interval	Tracked trajectory
$t_0 = 0\text{ s}$; $t_1 = 19\text{ s}$	Initial climb with rate of 10m/s and heading angle 0 (initial).
$t_1 = 19\text{ s}$; $t_2 = 29\text{ s}$	Vertical left helix towards the first waypoint. Rotation of 20° , rate of yaw of $2^\circ/\text{s}$ and a rate of climb of 10m/s. the turn radius is 1432 meters.
$t_2 = 29\text{ s}$; $t_3 = 290\text{ s}$	Climb with a rate of 10m/s until the time $t_h = 240\text{ s}$ (corresponds to $H=2400\text{ m}$) then a horizontal straight line.
$t_3 = 290\text{ s}$; $t_4 = 365\text{ s}$	A horizontal right level turn towards the second waypoint. The turn radius is 1432m and the yaw rate is $2^\circ/\text{s}$.
$t_4 = 365\text{ s}$; $t_5 = 660\text{ s}$	Horizontal straight line towards the second waypoint (5 km north et 10 km East).
$t_5 = 660\text{ s}$; $t_6 = 697\text{ s}$	Horizontal left level turn towards the target point
$t_6 = 697\text{ s}$; $t_7 = 993\text{ s}$	Straight line towards the target point (15km North and 25km East).
$t_7 = 993\text{ s}$; $t_8 = 1023\text{ s}$	Horizontal Right level turn. Rotation of 60° with yaw rate of $2^\circ/\text{s}$.
$t_8 = 1023\text{ s}$; $t_9 = 1173\text{ s}$	Horizontal left level turn of at least 300° around the target point (possibility of several rotations).
$t_9 = 1173\text{ s}$; $t_{10} = 1203\text{ s}$	Horizontal right level turn. Rotation of 60° to align on the trajectory which carries out towards the take-off/landing area.

km North and 10 km East for the second. In Fig. 9, the blue curve represents the UAV flight path. Table 4 presents the different phases of the mission with the transitions times between the different elementary trajectories.

IV. Conclusion

This paper presents an optimal trajectory planner algorithm for a fixed wing aerial vehicle, based on trim trajectories and Bang-Zero-Bang strategy. The trim trajectories particularity reduces significantly the complexity of the UAV dynamic model and thus the resolution of the trajectory tracking problem. The algorithm uses five trim trajectories as primitives: the horizontal, climb, descent wings-level flights, the level turn flight and the vertical helices with constant curvature and rate of climb. We demonstrate that the Bang-Zero-Bang strategy satisfies the optimality necessary condition of Pontryaguin. A numerical algorithm is presented for computing state and control vectors for different trim trajectories. The limitation of this algorithm is that the UAV airspeed is considered constant and constant during all elementary trajectories. Future work will allow a specific speed for each phase of flight. We will also introduce the wind effect in trajectory planning.

References

- [1] D. Boukraa, Y. Bestaoui, N. Azouz "A New Approach To Trajectories Planner Design For a Subsonic Autonomous Aerial Fixed Wing Vehicle", *American Control Conference*, Minneapolis, MN, 2006.
- [2] N. Faiz, S. Agrawal, R. Murray "Trajectory Planning of Differentially Flat Systems with Dynamics and Inequalities", *AIAA Journal of Guidance, Control, and Dynamics*, Vol. 24, No. 2, 2001.

- [3] J. How, E. King, Y. Kuwata “Flight Demonstrations of Cooperative Control for UAV Teams”, *AIAA 3rd Unmanned Unlimited Technical Conference*, 2004, Chicago, IL.
- [4] S. Jeyaraman et al, “Formal Techniques for the Modeling and Validation of a Co-Operating UAV Team That Uses Dubins Set For Path Planning”, *American Control Conference, 2005*, Portland, OR, pp. 4690-4695.
- [5] J. Spinkle, J. Eklund, S. Sastry “Deciding to Land a UAV Safely in Real Time”, *American Control Conference, 2005*, Portland, OR, USA.
- [6] G. Yang, V. Kapila “Optimal Path Planning for Unmanned Air Vehicles with Kinematic and Tactical Constraints”, *41st IEEE Conference on Decision and Control*, Las Vegas, NV, 2002.
- [7] M. Milam “Real-Time Optimal Trajectory Generation for Constrained Dynamical Systems”, *PhD Thesis, California Institute of Technology*, Pasadena, CA, 2003.
- [8] S. Hima, Y. Bestaoui, “Time Optimal Path Planning for an Underactuated Airship”, *proceedings of the AIAA Control and Guidance conference*, Austin, TX, 2003.
- [9] J. Marsden, T. Ratiu “Introduction to Mechanics and Symmetry”, *Springer, second edition*, 1999.
- [10] M. Van Nieuwstadt “Trajectory Generation for Nonlinear Control Systems”, *PhD Thesis, California Institute of Technology*, Pasadena, California, 1996.
- [11] M. Rathinam, R. Murray “Configuration Flatness of Lagrangian Systems Underactuated by one Control”, *IEEE Control and Decision Conference*, 1996.
- [12] S. Lavalle “Planning Algorithms”, *Cambridge University press*, 2006
- [13] S. Hansen, T. McLain, M. Goodrich ‘Probabilistic searching using a small unmanned aerial vehicle’, *AIAA Infotech@aerospace conference*, 2007, Rohnert Park, Ca.
- [14] L. Dubins “On curves of minimal length with a constraints with a constraint on average curvature and with prescribed initial and terminal positions and tangents”, *American Journal of Mathematics*, Vol. 79, pp 497-516, 1957.
- [15] P. Chandler, M. Pachter, S. Rasmussen, S., “UAV Cooperative Control”, *American Control Conference*, Arlington, VA, 2001.
- [16] E. Anderson, R. Beard, T. McLain “Real Time Dynamic Trajectory Smoothing for Unmanned Air Vehicles”, *IEEE Transactions on Control Systems Technology*, Vol. 13, 2005.
- [17] D. Boukraa, Y. Bestaoui, N. Azouz “Trajectories characterization of an autonomous aerial vehicle with a small angle of attack”, *23rd Digital Avionics Systems Conference*, Salt Lake City, Utah, 2004
- [18] D. Boukraa, Y. Bestaoui, N. Azouz “Transition Trajectories Characterization for Uninhabited aerial Vehicle”, *24th Digital Avionics Systems Conference*, Washington D.C., 2005
- [19] D. Boukraa, Y. Bestaoui, N. Azouz “Non Trim trajectories Characterization Of An Unmanned Aerial Fixed Wing Vehicle”, *11th IEEE International conference on Methods and Models in Automation and Robotics*, 2005, Miedzyzdroje, Poland.
- [20] B. Stevens, F. Lewis “Aircraft Control and Simulation”, *Editions Wiley Interscience*, 2003.

λ	=	Lagrange multiplier
θ	=	pitch angle
Π	=	throttle control
$\vec{\omega}$	=	angular velocity vector $(p \ q \ r)^T$
ψ	=	yaw (heading) angle.
f_i	=	generic functions
p_i	=	i^{th} waypoint
H	=	Hamiltonian function
J	=	performance index
R	=	the turn flight radius
U	=	control vector $(\Pi \ \delta_e \ \delta_a \ \delta_r)^T$
\vec{V}	=	linear velocity vector $(u \ v \ w)^T$.
V	=	Vehicle airspeed.
X	=	state vector $(V \ \alpha \ \beta \ p \ q \ r)^T$ or $(u \ v \ w \ p \ q \ r)^T$

NOMENCLATURE

α	=	angle of attack
β	=	sideslip angle
δ_e	=	elevator deflection angle
δ_a	=	aileron deflection angle
δ_r	=	rudder deflection angle
ρ	=	generic parameter
τ	=	generic parameter
ϕ	=	roll angle
γ	=	Flight path angle